NMR Spectroscopy Hot Paper

DOI: 10.1002/anie.201403416

Ultra-Low-Field NMR Relaxation and Diffusion Measurements Using an Optical Magnetometer**

Paul J. Ganssle, Hyun D. Shin, Scott J. Seltzer, Vikram S. Bajaj, Micah P. Ledbetter, Dmitry Budker, Svenja Knappe, John Kitching, and Alexander Pines**

Abstract: *Nuclear magnetic resonance (NMR) relaxometry and diffusometry are important tools for the characterization of heterogeneous materials and porous media, with applications including medical imaging, food characterization and oil-well logging. These methods can be extremely effective in applications where high-resolution NMR is either unnecessary, impractical, or both, as is the case in the emerging field of portable chemical characterization. Here, we present a proof-of-concept experiment demonstrating the use of high-sensitivity optical magnetometers as detectors for ultra-low-field NMR relaxation and diffusion measurements.*

Nuclear magnetic resonance (NMR) relaxometry and diffusometry are important tools for the characterization of heterogeneous materials and porous media,[1] with applications including the study of biological systems,[2,3] medical imaging, food characterization,[4,5] and oil-well logging.[6,7] These methods can be extremely effective in applications where high-resolution NMR is either unnecessary, impractical, or both. The pulse sequences used to make these measurements are often robust even in the presence of sample motion, strong gradients, and pulse imperfections,[8,9] allowing for the use of magnetic resonance in extreme environments or under conditions with rigid design constraints. Relaxometry and diffusometry are often used when making ex-situ measurements, wherein the geometry of the usual NMR experiment is inverted and a detector is used to either probe the surface of a larger sample or it is entirely surrounded by the sample.[10–12] In these cases, the volume and geometry within which it is possible to create a homogeneous field are limited, and in general it is not feasible to generate the field strengths necessary to make high resolution NMR measurements; however, relaxation and diffusion depend on many environmental factors including chemical composition, pressure,[13] temperature,[14,15] phase,[16,17] and even sample geometry,[18] and as such measurements of these processes can yield considerable information about the sample.

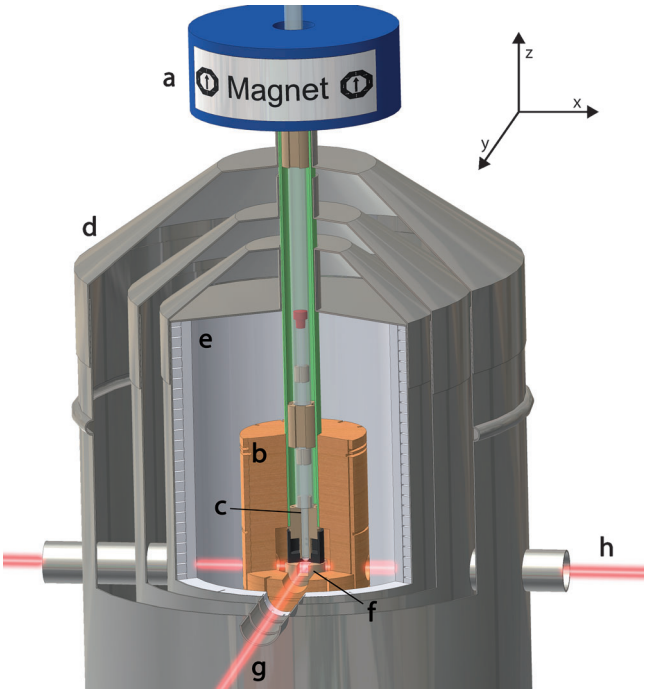

Figure 1. The sample is shuttled between a 2 T pre-polarizing magnet (a) and the zero-field detection region. Pulses are applied using a set of four coils wound around a 3D-printed substrate (b) centered on the sample (c), which is contained in a standard 5 mm NMR tube. External fields are removed using μ-metal shielding (d) and the detection region is shimmed to zero field using a set of coils wound on a Teflon substrate (e). The rubidium spins in the spin exchange relaxation-free cell (f) are polarized along the *y* axis by a circularly polarized pump beam (g), and their precession in the presence of a magnetic field along the *z* axis is detected by measuring optical rotation of the linearly-polarized probe beam propagating along *x* (h).

[*] P. J. Ganssle, H. D. Shin, Dr. S. J. Seltzer, Dr. V. S. Bajaj, Prof. A. Pines
Department of Chemistry, University of California
Berkeley, CA 94720 (USA)
and
Material Science Division, Lawrence Berkeley National Labs
Berkeley, CA 94720 (USA)
E-mail: pganssle@berkeley.edu
pines@berkeley.edu
Dr. M. P. Ledbetter, Prof. D. Budker
Department of Physics, University of California
Berkeley, CA 94720 (USA)
Prof. D. Budker
Nuclear Science Division, Lawrence Berkeley National Labs
Berkeley, CA 94720 (USA)
Dr. S. Knappe, Dr. J. Kitching
Time and Frequency Division, National Institute of Standards and Technology
Boulder, CO 80305 (USA)

[**] This work was supported by the Director, Office of Science, Office of Basic Energy Sciences, Materials Sciences and Engineering Division, of the U.S. Department of Energy under Contract DE-AC02-05CH11231 (instrument fabrication and salaries for P.J.G., H.D.S., S.J.S. and A.P.) and by the Innovation Grant Program of Lawrence Berkeley National Labs under U.S. Department of Energy Contract No. DE-AC02-05CH11231 (salary for SJS). This work is a partial contribution of NIST, an agency of the US government, and is not subject to copyright in the United States.

Here, we demonstrate that advances in magnetometer technology can help to alleviate at least one of the challenges related to ex-situ NMR measurements—the difficult problem of generating a homogeneous field over a sufficiently large sample area. In traditional, coil-based NMR, detector sensitivity is directly proportional to frequency, and thus the magnetic field strength—necessitating the use of a powerful magnet to induce a bias offset, which inherently limits the homogeneity of any ex-situ measurement, as well as the depth to which a sample can be probed. On the other hand, at low frequencies, the sensitivity of an atomic magnetometer is roughly independent of the frequency[19] (and thus magnetic field), allowing measurements to be made in the Earth's ambient magnetic field, which can be homogeneous over even large samples (typical inhomogeneities are on the order of 1 ppm over a cm^3 volume).[20]

Alkali-vapor-cell magnetometers[21] are strong candidates for use as sensors in a portable, low-field NMR device: they are relatively inexpensive, low-maintenance, low power, robust to temperature, pressure and vibration, and can be microfabricated and as such can be integrated into compact sensor arrays. They are also among the most sensitive magnetic field sensors currently available,[22] and have already been used to demonstrate measurements of NMR at low and zero field,[23–25] as well as measurements of sample relaxation in the presence of gadolinium contrast agents.[26]

Here we demonstrate for the first time that with a high-sensitivity optical magnetometer, one can to chemically resolve a heterogeneous mixture of hydrocarbon solvents and water by their relaxation and diffusion properties, both in one-dimensional experiments and in two-dimensional correlation experiments. This represents a significant step towards the use of atomic magnetometry in wider industrial applications, and a proof-of-concept for a potentially powerful next generation of portable NMR sensors.

Magnetic resonance signals were detected at zero field using a shielded rubidium vapor-cell magnetometer with a $5 \times 5 \times 10$ mm glass cell (Figure 1 f) at 200 torr N_2 buffer gas operating at 155 °C; due to the elevated temperature in proximity to the sensor, samples were cooled to 37 °C by flowing dry N_2 gas over them. Samples in standard 5 mm NMR tubes (Figure 1 c) were prepolarized in a 2 T permanent magnet (Figure 1 a) outside the magnetic shields (Figure 1 d) and pneumatically shuttled into the detection region in approximately 700 ms, which effectively acted as a 700 ms T_1 filter; this does not significantly affect the measurements of the samples of interest in these experiments, as the T_1 of nearly all components is ≥ 1 s, and so signal decay is acceptable on this time scale. The detection region is shimmed to zero field using a tri-axial set of coils wound on a PTFE (polytetrafluoroethylene) substrate inside the innermost shield (Figure 1 e). A second, smaller set of coils wound on a 3D-printed plaster substrate (Figure 1 b) is used to apply field and gradient pulses to the sample.

Our magnetometer uses a spin exchange relaxation-free (SERF) configuration,[22,27] which has optimal response at zero field, and as such all low-field experiments are performed in an indirect, field-cycled dimension. Although magnetometers can be configured to operate at Earth's field with comparable sensitivity,[21] a field-cycled experiment was chosen to allow maximum versatility in choice of the bias field during relaxation—because the strength of the B_z bias field is independent of the field during detection and pulsing, the device does not need to be re-tuned when the bias field is changed. In these experiments, a Helmholtz coil is used to generate a B_z field of 0.5 G, to emulate the Earth's ambient magnetic field, and this field is switched off while applying rotation pulses and making measurements (Figure 2). Magnetization signal is measured by applying a train of π pulses to the spins and taking the average magnitude of change in magnetometer signal in response to a π pulse—a measure taken to mitigate the effects of drift and other low-frequency signal artifacts.

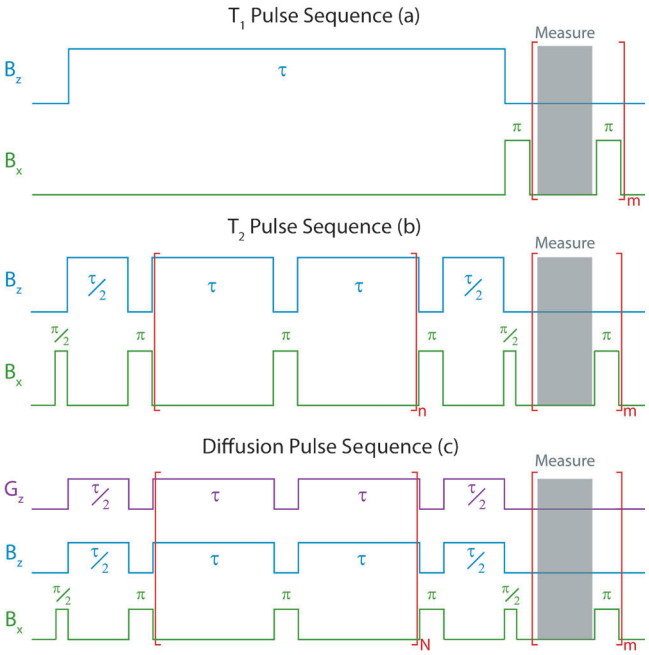

Figure 2. a) Since spins are pre-polarized, T_1 is measured by observing the polarization equilibrate in the chosen B_z field. b) T_2 is measured by observing the magnitude of subsequent echos in a CPMG train. c) The diffusion coefficient is measured by varying the strength of the gradient G_z with a fixed number of CPMG lobes (N). In all sequences, the signal is measured between a sequence of π pulses to distinguish between background fields and NMR signal.

Relaxation and diffusion were measured using the pulse sequences detailed in Figure 2. Because the pre-polarized spins are equilibrating to a near-zero polarization state at 0.5 G, rather than using an inversion–recovery or saturation–recovery sequence, the longitudinal relaxation time (T_1) is measured as an exponential decay of the spin magnetization as a function of an increasing delay time between the sample pre-polarization and measurement. The transverse relaxation time (T_2) is measured using a standard Carr–Purcell–Meiboom–Gill (CPMG) spin–echo–train pulse sequence with the bias field set at 0.5 G during the inter-pulse delay time and at 0 G during the pulses so that DC pulses can be used to tip the spins, wherein the inter-pulse spacing (τ) is held constant and the number of pulses (n) is varied; as the effects of convection

and other forms of coherent motion are eliminated on alternate echoes,[28] only even echoes were measured. Diffusion was measured using a CPMG pulse sequence in the presence of a gradient[29] which was switched on during the inter-pulse delays, however, both τ and N were kept at fixed values and the gradient strength (G) was increased, to eliminate any effects not directly related to diffusion. Magnetization signal generated as a result of these pulse sequences have the form:

$$M_{T_1}(\tau) = M_0\, e^{-\tau/T_1} \tag{1}$$

$$M_{T_2}(n,\tau) = M_0\, e^{-n\tau/T_2} \tag{2}$$

$$M_D(G,\tau,N) = M_0\, e^{-N\tau/T_2}\, e^{-(\gamma\tau G)^2 N\tau D/3} \tag{3}$$

For simple single-component signals, a least-squares fit to the appropriate kernel function was sufficient to characterize the system accurately. For more complicated experiments, the pseudo-spectrum $F(x)$ in the domain of the parameter of interest was generated from the magnetization signals $M(\tau)$ by solving the relevant Fredholm integral of the first kind for the appropriate kernel functions $k(\tau,x)$:[30,31]

$$M(\tau) = \int k(\tau,x)F(x)\mathrm{d}x. \tag{4}$$

This extends to two-dimensional correlation spectra:

$$M(\tau_1,\tau_2) = \int\int k_1(\tau_1,x)k_2(\tau_2,y)F(x,y)\mathrm{d}x\mathrm{d}y. \tag{5}$$

These are well-known to be ill-posed problems,[32] giving results which are sensitive to error in the data, and so the inversion was performed using a MATLAB toolkit with SVD (singular value decomposition) truncation and Tikhonov regularization based on the procedures detailed in Venkataramanan et al.[31] and Mitchell et al.[33]

We made measurements of the relaxation properties of water and a series of common hydrocarbons at 0.5 G, demonstrating clearly that the chemical sensitivity of this technique is sufficient to distinguish between water and hydrocarbons (Table 1), both from their T_1/T_2 ratio and by the values of T_1 and T_2, which had single-transient fit errors on the order of 5%. It is worth noting that both the T_1 and T_2 times of water are very sensitive to temperature;[14,15] because of the sample proximity to the hot magnetometer cell, most measurements were taken at an elevated temperature. It was not possible to experimentally determine the temperature gradient across the sample in-situ, but the relatively narrow T_1, T_2 and diffusion coefficient distributions (as can be seen in Figure 4) suggest a low temperature gradient in the region of interest. Generally the samples were air-cooled to 37 °C during measurements, but there is some variation in the measurement temperature due to changes in the magnetometer configuration. The relaxation constants of water at near-zero field are strongly dependent on B_z,[34] and so care was taken to make measurements only at 0.5 G, with an aim to best emulate the Earth's field.

As an artifact of the ex-situ geometry of the experimental setup, spins at the bottom of the sample tube contribute to the

Table 1: Relaxation times of some common solvents measured at 0.5 G, 37 °C.

Compound	T_1 [s]	T_2 [s]
water	3.27 ± 0.15	2.08 ± 0.13
methanol	2.88 ± 0.08	2.50 ± 0.05
ethanol	2.07 ± 0.06	2.07 ± 0.06
hexadecane	0.75 ± 0.03	0.65 ± 0.02
limonene	1.62 ± 0.04	1.40 ± 0.10
heptane	1.91 ± 0.04	1.70 ± 0.07
octane	1.83 ± 0.08	1.67 ± 0.03
decane	1.56 ± 0.07	1.32 ± 0.08

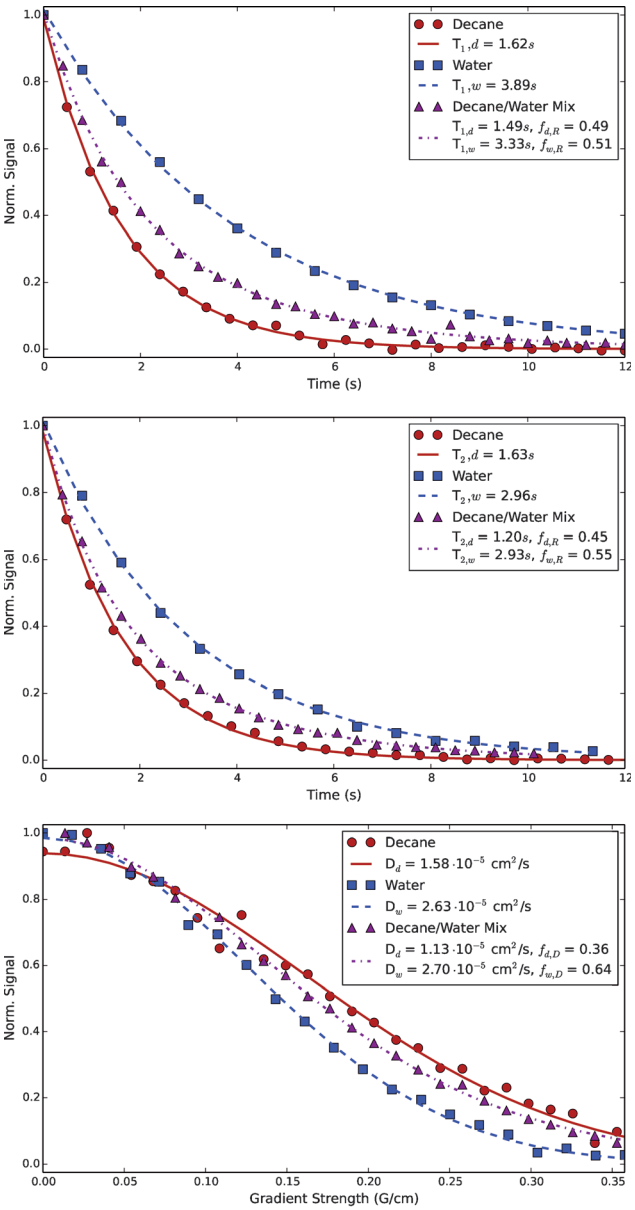

Figure 3. Acquisition of the T_1 (top), T_2 (middle) and diffusion measurements (bottom) of decane, water and a mixture of decane and water, fit with least-squares fitting to the relevant kernel functions.

magnetometer signal more strongly than spins towards the top. This can cause problems when attempting to make measurements of immiscible liquids, as signal from the denser component will tend to dominate the less dense component as the fluids separate out. In order to make accurate measurements of signal from immiscible liquids, samples were physically separated using a coaxial insert which separated liquid in a smaller, 3.3 mm NMR tube from the liquid in a standard thin-walled 5 mm NMR tube. Using this method, T_1, T_2 and diffusion were measured in decane, water and a decane/water mixture to demonstrate that atomic magnetometers have the sensitivity required to quantitatively separate components from heterogeneous mixtures at 0.5 G.

Due to the pre-polarization and shuttling steps, the fraction of signal generated by each component in these experiments must be adjusted for T_1 relaxation during shuttling. For the relaxation experiments, the signal fraction for a component c ($f_{c,R}$) is a function of the hydrogen density ($\rho_{H,c}$), volume (V_c), shuttling time (t_s), and the component T_1 relaxation time ($T_{1,c}$):

$$f_{c,R} = \frac{\rho_{H,c} \cdot V_c \cdot e^{-t_s/T_{1,c}}}{\sum_i \rho_{H,c} \cdot V_{c_i} \cdot e^{-t_s/T_{1,c_i}}}. \quad (6)$$

And in diffusion experiments, it is also necessary to take into account the T_2 decay during the diffusion sequence itself:

$$f_{c,D} = \frac{\rho_{H,c} \cdot V_c \cdot e^{-t_s/T_{1,c}} \cdot e^{-2n\tau/T_{2,c}}}{\sum_i \rho_{H,c_i} \cdot V_{c_i} \cdot e^{-t_s/T_{1,c_i}} \cdot e^{-2n\tau/T_{2,c_i}}}. \quad (7)$$

The volumes for the decane in the inner tube and water in the outer tube were $V_d = 53 \pm 1$ μL and $V_w = 59 \pm 1$ μL, respectively, and the diffusion measurements were made with $N = 6$ and $\tau = 75$ ms. As $\rho_{H,d} = 112.95$ M and $\rho_{H,w} = 110$ M, the expected value for $f_{d,R}$ is 0.42 ± 0.01 and the expected value of $f_{d,D}$ is 0.36 ± 0.01. The experimental results shown in Figure 3 of $f_{d,T_1} = 0.48 \pm 0.04$, $f_{d,T_2} = 0.45 \pm 0.04$ and $f_{d,D} = 0.36$, agree with these predictions, which clearly demonstrates that not only is this technique chemically sensitive, but can be used for fairly accurate quantification of the components of a heterogeneous mixtures.

These same techniques were also extended to acquire the two-dimensional T_1–T_2 (Figure 4a) and T_2-diffusion (Figure 4b) correlation spectra—both experiments widely used in industrial applications. The data plotted in Figure 4 show clearly separated peaks corresponding to decane and water. As these data were acquired over a long time period (12–36 h), drift was a significant concern, and so experiments were acquired without active cooling to avoid potential temperature instabilities due to changes in the N_2 backpressure over the course of the day—for consistency, the data presented in Figure 3 were also performed without active cooling. Due to uncorrected drift over the course of the experiments, minor fast-relaxing artifacts appear in the diffusion-T_2 Laplace pseudospectrum; these artifacts do not significantly affect the results and are likely unique to this experimental configuration.

These experiments, which demonstrate that atomic magnetometers have sufficient sensitivity to perform industrially relevant NMR measurements for the characterization of hydrocarbon/water mixtures at low field, are an important first step towards the development of compact, inexpensive devices which can take advantage of the Earth's highly homogeneous ambient magnetic field. Many of the limitations present in these experiment—the instrument configuration, elevated temperature and measurement at zero field most notable among them—are artifacts of the design of the

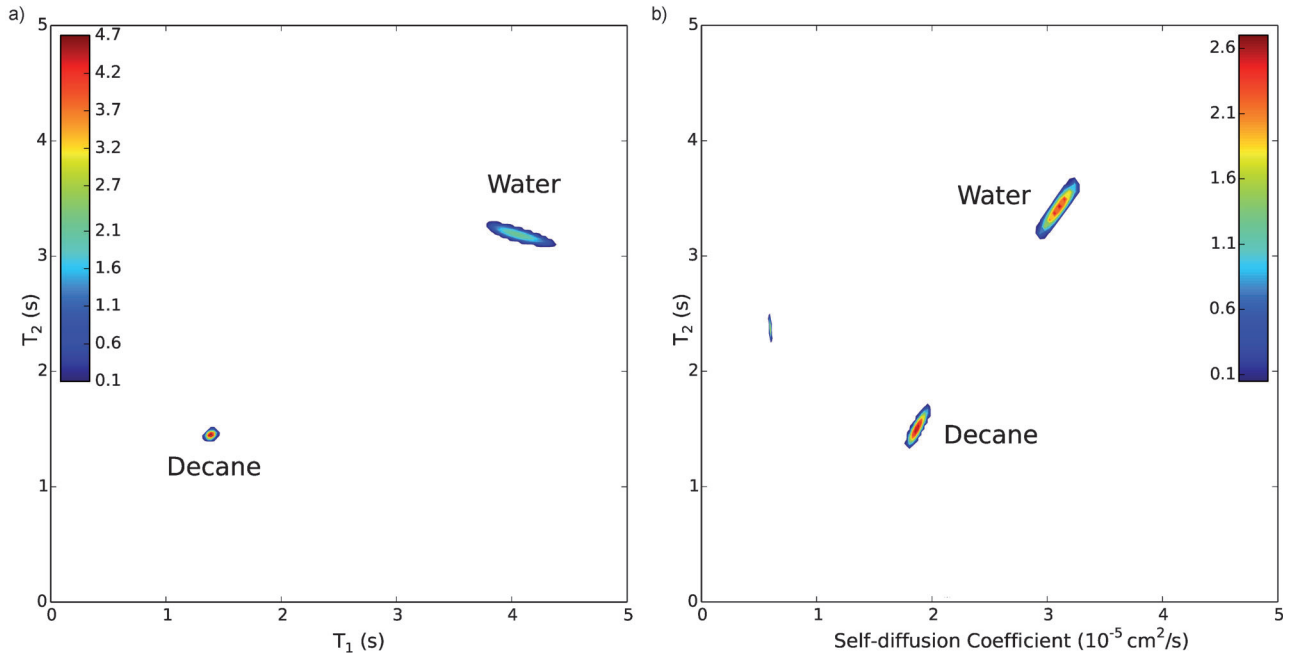

Figure 4. a) T_1–T_2 and b) T_2-diffusion Laplace pseudospectra of decane and water. The extra peak in the T_2-diffusion spectrum is an artifact of the inversion procedure used. The colors in the figure correspond to relative intensity, normalized to 100.

device a versatile low-field sensor and can be avoided in a more specialized context. The strength of these results in spite of such limitations show that these experiments are a critical step towards the realization of the promise that optical, non-cryogenic magnetometers show as a low-cost, portable, robust NMR sensor, and makes a compelling case for future research into their implementation in the fields of medical imaging, explosives detection, materials characterization and particularly oil-well logging.

Received: March 31, 2014
Published online: July 31, 2014

Keywords: analytical methods · low-field NMR spectroscopy · optical magnetometry · sensors

[1] Y.-Q. Song in *NMR Imaging in Chemical Engineering*, 1st ed. (Eds.: S. Stapf, S.-I. Han), Wiley-VCH, Weinheim, **2006**, chap. 2.7.1, pp. 163 – 182.
[2] J. G. Seland, M. Bruvold, H. Anthonsen, H. Brurok, W. Nordhøy, P. Jynge, J. Krane, *Magn. Reson. Imaging* **2005**, *23*, 353 – 354.
[3] M. Köpf, C. Corinth, O. Haferkamp, T. Nonnenmacher, *Biophys. J.* **1996**, *70*, 2950 – 2958.
[4] M. D. Hürlimann, L. Burcaw, Y.-Q. Song, *J. Colloid Interface Sci.* **2006**, *297*, 303 – 311.
[5] A. Guthausen, G. Guthausen, A. Kamlowski, H. Todt, W. Burk, D. Schmalbein, *J. Am. Oil Chem. Soc.* **2004**, *81*, 727 – 731.
[6] R. L. Kleinberg, J. A. Jackson, *Concepts Magn. Reson.* **2001**, *13*, 340 – 342.
[7] M. D. Hürlimann in *Encyclopedia of Magnetic Resonance*, Wiley, Hoboken, **2012**.
[8] M. D. Hürlimann, D. D. Griffin, *J. Magn. Reson.* **2000**, *143*, 120 – 135.
[9] M. D. Hürlimann, *J. Magn. Reson.* **2001**, *148*, 367 – 378.
[10] B. Blümich, P. Blümler, G. Eidmann, R. Savelsberg, A. Guthausen, R. Haken, U. Schmitz, K. Saito, G. Zimmer, *Magn. Reson. Imaging* **1998**, *16*, 479 – 484.
[11] *Single-Sided NMR* (Eds.: F. Casanova, J. Perlo, B. Blümich), Springer, Heidelberg, **2011**.
[12] J. A. Jackson, L. J. Burnett, J. F. Harmon, *J. Magn. Reson.* **1980**, *41*, 411 – 421.
[13] T. Defries, J. Jonas, *J. Chem. Phys.* **1977**, *66*, 896 – 901.
[14] J. H. Simpson, H. Y. Carr, *Phys. Rev.* **1958**, *111*, 1201 – 1202.
[15] P. J. M. van Bentum, G. H. A. van der Heijden, J. A. Villanueva-Garibay, A. P. M. Kentgens, *Phys. Chem. Chem. Phys.* **2011**, *13*, 17831 – 17840.
[16] E. L. Rumeur, J. de Certaines, P. Toulouse, P. Rochcongar, *Magn. Reson. Imaging* **1987**, *5*, 267 – 272.
[17] H. A. Resing, *J. Chem. Phys.* **1965**, *43*, 669 – 678.
[18] L. van der Weerd, S. M. Melnikov, F. J. Vergeldt, E. G. Novikov, H. V. As, *J. Magn. Reson.* **2002**, *156*, 213 – 221.
[19] I. M. Savukov, S. J. Seltzer, M. V. Romalis, *J. Magn. Reson.* **2007**, *185*, 214 – 220.
[20] S. Appelt, H. Kühn, F. W. Häsing, B. Blümich, *Nat. Phys.* **2006**, *2*, 106 – 109.
[21] D. Budker, M. Romalis, *Nat. Phys.* **2007**, *3*, 227 – 234.
[22] I. K. Kominis, T. W. Kornack, J. C. Allred, M. V. Romalis, *Nature* **2003**, *422*, 596.
[23] M. P. Ledbetter, I. M. Savukov, D. Budker, V. Shah, S. Knappe, J. Kitching, D. J. Michalak, S. Xu, A. Pines, *Proc. Natl. Acad. Sci. USA* **2008**, *105*, 2286 – 2290.
[24] T. Theis, P. J. Ganssle, G. Kervern, S. Knappe, J. Kitching, M. P. Ledbetter, D. Budker, A. Pines, *Nat. Phys.* **2011**, *7*, 571 – 575.
[25] M. P. Ledbetter, T. Theis, J. W. Blanchard, H. Ring, P. J. Ganssle, S. Appelt, B. Blumich, A. Pines, D. Budker, *Phys. Rev. Lett.* **2011**, *107*, 107601.
[26] D. J. Michalak, S. Xu, T. J. Lowery, C. W. Crawford, M. Ledbetter, L. S. Bouchard, D. E. Wemmer, D. Budker, A. Pines, *Magn. Reson. Med.* **2011**, *66*, 603 – 606.
[27] I. Savukov, S. J. Seltzer in *Optical Magnetometry* (Eds.: D. Budker, D. F. J. Kimball), Cambridge University Press, 1edst ed**2013**, chap. 5, pp. 85 – 103.
[28] H. Y. Carr, E. M. Purcell, *Phys. Rev.* **1954**, *94*, 630 – 638.
[29] E. Fukushima, S. B. W. Roede, *Experimental Pulse NMR* **1993**, 197 – 201.
[30] Y.-Q. Song, L. Venkataramanan, M. D. Hürlimann, M. Flaum, P. Frulla, C. Straley, *J. Magn. Reson.* **2002**, *154*, 261 – 268.
[31] L. Venkataramanan, Y.-Q. Song, M. D. Hürlimann, *IEEE Trans. Signal processing* **2002**, *50*, 1017 – 1026.
[32] J. P. Butler, J. A. Reeds, S. V. Dawson, *SIAM J. Numerical Anal.* **1981**, *18*, 381 – 397.
[33] J. Mitchell, T. C. Chandrasekera, L. F. Gladden, *Prog. Nucl. Magn. Reson. Spectrosc.* **2012**, *62*, 34 – 50.
[34] S. Hartwig, J. Voigt, H.-J. Scheer, H.-H. Albrecht, M. Burghoff, L. Trahms, *J. Chem. Phys.* **2011**, *135*, 054201.

